

Nonlinear Chemical Imaging Microscopy: Near-Field Third Harmonic Generation Imaging of Human Red Blood Cells

Richard D. Schaller, Justin C. Johnson, and Richard J. Saykally*

Department of Chemistry, University of California, Berkeley, California 94720

Third harmonic generation (THG) imaging using a near-field scanning optical microscope (NSOM) is demonstrated for the first time. A femtosecond, tunable near-infrared laser was used to generate both nonresonant and resonantly enhanced third harmonic radiation in human red blood cells. We show that resonantly enhanced THG is a chemically specific bulk probe in NSOM imaging by tuning the excitation source onto and off of resonance with the Soret transition of oxyhemoglobin. Additionally, we provide evidence that tightly focused, nonresonant, far-field THG imaging experiments do not produce contrast that is truly surface specific.

There is much current interest in the use of third harmonic generation (THG) as a microscopy tool.^{1–5} It has been shown that third harmonic generation becomes a surface-selective probe when a sample is excited at very high laser intensities and far away from molecular resonances. As a new far-field microscopy contrast mechanism, its utility is quite apparent. Under tight focusing conditions, it appears that the presence of surfaces increases THG efficiency making, for example, transparent cellular organelles and damage spots inside of glass readily observable.^{6,7} Such features are difficult to image with more traditional microscopies as they have no visible color and are nonfluorescent. It is the intent of this work to explore the potential of THG as a novel contrast mechanism for near-field imaging. Near-field THG should exhibit characteristics different from those of far-field experiments, primarily due to the relaxation of phase-matching conditions inherent in nonlinear optical near-field scanning optical microscope (NSOM) techniques.^{8,9}

Conventional wisdom holds that even-order nonlinear optical processes are typically surface specific while odd-order processes

are predominantly bulk probes.¹⁰ Second harmonic generation (SHG) can be produced only in materials that lack an inversion center under the dipole approximation, as this condition is explicitly required for $\chi^{(2)}$ to be nonvanishing. As all interfaces necessarily lack an inversion center, SHG can provide monolayer-sensitive chemical information when the bulk is isotropic. This selection rule involves molecular and translational symmetry elements that are microscopic in nature, as opposed to the phase-matching condition, which is a far-field propagation requirement. Therefore, near-field detected SHG can remain explicitly surface selective when the sample bulk is isotropic. In comparison, THG can be produced from all materials independent of centrosymmetry, because it is dipole allowed. Both surface and bulk molecules will produce third harmonic light, with the bulk typically producing orders of magnitude more signal simply due to the response of more molecules.¹⁰ Within these considerations, $\chi^{(3)}$ is not intrinsically surface sensitive in the same manner as is SHG.

The third-order polarizability induced in a sample is described by the equation^{10,12}

$$P_i^{(3)}(3\omega) \propto \chi_{ijkl}^{(3)} E(\omega_j) E(\omega_k) E(\omega_l) \quad (1)$$

where $\chi_{ijkl}^{(3)}$ is a fourth rank tensor that describes the coupling of the three electric fields, $E(\omega_{j,k,l})$, to create the third harmonic polarization, and i, j, k , and l are electric field orientations with respect to laboratory coordinates. $\chi^{(3)}$, in direct analogy to $\chi^{(2)}$, consists of both nonresonant and resonant terms

$$\chi_{\text{total}}^{(3)} = \chi_{\text{NR}}^{(3)} + \chi_{\text{R}}^{(3)} \quad (2)$$

where the resonant term can be described by

$$\chi_{ijkl}^{(3)}(-3\omega, \omega, \omega, \omega) \approx \sum_{n, n', n'' \neq g} \frac{\langle g | i | n \rangle \langle n | j | n' \rangle \langle n' | k | n'' \rangle \langle n'' | l | g \rangle}{(2\omega - \omega_{n'g} + i\Gamma_{n'g})(\omega - \omega_{ng} + i\Gamma_{ng})} \times \text{permutations} \quad (3)$$

* Corresponding author. E-mail: saykally@cchem.berkeley.edu.

- (1) Tsang, T. Y. F. *Phys. Rev. A* **1995**, 52, 4116–25.
- (2) Barad, Y.; Eisenberg, H.; Horowitz, M.; Silberberg, Y. *Appl. Phys. Lett.* **1997**, 70, 922–4.
- (3) Squier, J. A.; Muller, M.; Brakenhoff, G. J.; Wilson, K. R. *Opt. Express* **1998**, 3, 315–24.
- (4) Yelin, D.; Silberberg, Y. *Opt. Express* **1999**, 5, 169–75.
- (5) Yelin, D.; Silberberg, Y.; Barad, Y.; Patel, J. S. *Appl. Phys. Lett.* **1999**, 74, 3107–9.
- (6) Muller, M.; Squier, J. A.; Wilson, K. R.; Brakenhoff, G. J. *J. Microsc.* **1998**, 191, 266–74.
- (7) Squier, J. A.; Muller, M. *Appl. Opt.* **1999**, 38, 5789–94.
- (8) Zhao, X.; Kopelman, R. *Ultramicroscopy* **1995**, 61, 69–80.
- (9) Vigoureux, J. M.; Girard, C.; Depasse, F. *J. Mod. Opt.* **1994**, 41, 49–58.

(10) Shen, Y. R. *Principles of Nonlinear Optics*; Wiley: New York, 1984.

(11) Schaller, R. D.; Roth, C.; Raulet, D. H.; Saykally, R. J. *J. Phys. Chem. B* **2000**, 104, 5217–20.

(12) Boyd, R. *Nonlinear Optics*; Academic: New York, 1992.

and can dramatically increase THG signals when molecular transitions, ω_{ng} , $\omega_{n'g}$, and $\omega_{n'n'g}$, in the sample are approached by the experimental frequencies ω , 2ω , 3ω or combinations of these (single and multiple resonances, respectively). The dipole transition matrix elements, such as $\langle g|i|n\rangle$, indicate the coupling along the i coordinate between the ground state, g , and an excited state, n . The Γ^{-1} values are characteristic relaxation times for the corresponding molecular transitions. We have previously shown that the resonance-enhancement term of the second-order response could be used to perform NSOM imaging with both surface selectivity and chemical specificity.¹¹ The third-order response should demonstrate similar chemical specificity, although resonantly enhanced $\chi^{(3)}$ will probe both anisotropic and isotropic environments as it is dipole allowed.¹⁰

Recent work has established that THG can become surface selective when far from resonances and under tight focusing of the fundamental laser,¹⁻³ although the exact nature of the response and degree of surface selectivity is still uncertain. It was first suggested by Tsang that the surface selectivity may result from an intrinsic surface-enhanced $\chi^{(3)}$ effect, which would involve only a few monolayers, in direct analogy to surface-enhanced SHG.¹ Barad et al. have more recently proposed that the observed surface selectivity results from relaxation of phase-matching conditions at an interface due to the gradient in the refractive index and/or the third-order nonresonant susceptibility at an interface.² This mechanism does not invoke a surface-enhanced component of the $\chi^{(3)}$ response but is simply an extension of the work by Boyd¹² on the efficiency of bulk THG using focused Gaussian beams. Barad's mechanism would present a THG probe depth determined by the confocal properties of the laser. This depth is typically several hundreds of nanometers to micrometers, or thousands of monolayers, in the tightly focused limit.

These two very different proposed mechanisms of surface-selective far-field THG can be tested with THG NSOM experiments, as the phase-matching condition is relaxed a priori when a probe collects the signal before interference effects of propagation have occurred. If a surface-enhanced component of the total $\chi^{(3)}$ is the mechanism by which surface selectivity is effected, near-field THG experiments would maintain surface specificity, as such an intrinsic mechanism should be independent of the optical collection method. THG NSOM experiments would then produce results that are similar to tightly focused, far-field THG experiments, albeit with higher spatial resolution. If, instead, the source of surface-selective THG is relaxation of phase-matching conditions due to the interfacial change in refractive index or bulk $\chi^{(3)}$, then THG NSOM experiments should not be surface selective as the phase-matching condition should be relaxed at all subwavelength distances from the probe. Thus, detected signals would contain a very significant bulk contribution.

EXPERIMENTAL SECTION

The experimental design shown in Figure 1, which has been described in detail previously for near-field SHG experiments,¹¹ was used with only slight modification to measure the THG response of a sample. Near-field microscopy was performed using a commercial NSOM system (Thermomicroscopes, Lumina) that is equipped with a nonoptical tuning fork feedback mechanism

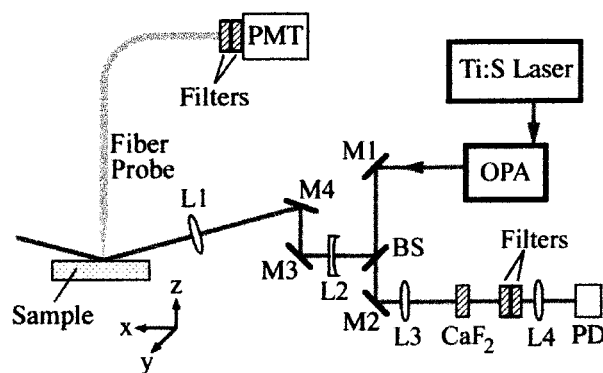


Figure 1. Experimental setup: Beam splitter (BS), 8 cm focal length plano-convex lens (L1), -5 cm focal length plano-concave lens, 5 cm focal length biconvex lens (L3), 2 cm focal length biconvex lens (L4), steering mirrors (M1-4).

that maintains the probe-sample distance at $\sim 5-10$ nm.¹³ Adiabatically pulled, uncoated, ~ 50 nm radius of curvature amorphous SiO_2 NSOM probes (characterized using scanning electron microscopy) were used for all THG experiments. Topographical and optical images were collected simultaneously.

A laser system consisting of a commercial (Quantronix) optical parametric amplifier (OPA), pumped by a chirped pulse amplified titanium:sapphire laser (Spectra-Physics) (800 nm, 2.5 W, 80 fs, 1 kHz) that was seeded with the output of a home-built titanium:sapphire oscillator (800 nm, 480 mW, 30 fs, 88 MHz), was used to generate tunable near-infrared wavelengths for the experiments ($1.1-2.7 \mu\text{m}$, 400 mW at $1.4 \mu\text{m}$, 70 fs, $\Delta\nu \sim 280 \text{ cm}^{-1}$). The fundamental beam was split 50:50 into a sample and reference arm. The p-polarized, $15 \mu\text{J}$ sample pulses were focused with a Galilean telescope to a $\sim (50 \mu\text{m})^2$ spot at the point where the NSOM probe investigated the sample. Light collected in the near-field was directed via the optical fiber to 505 nm short-pass filters and an R3896 Hamamatsu photomultiplier tube (PMT). The sample was scanned to maintain the laser-probe geometry and only examine one region of the laser spot. The reference pulses were focused into a 2 mm thick calcium fluoride window, filtered to pass only the third harmonic, and were measured with a silicon photodiode (PD). Separate optical images were collected during forward and reverse scans to check for image reproducibility. Repeatable forward and reverse scans were then added together to reduce noise. Each NSOM image in this work consists of a 200×200 pixel array, and each final THG pixel is the average of 40 laser shots. Signals collected by the near-field probe were also directed to a 0.3 m spectrograph (Acton Research), dispersed with a 150 grooves/mm grating, and detected with a CCD to produce THG NSOM spectra.

Human erythrocytes were dried from whole blood on a glass microscope slide using compressed air to spatially isolate cells. Erythrocytes contain a large amount of hemoglobin in the cytoplasm. The hemoglobin in the erythrocytes was in the oxygenated form as efforts were not made to isolate the sample from ambient oxygen. The Soret transition of oxyhemoglobin is very strong and has a $\lambda_{\text{max}} = 415 \text{ nm}$ ($\epsilon \sim 135 \text{ cm}^{-1}/\text{mM}$).¹⁴

(13) Ruiter, A. G. T.; Van Der Werf, K. O.; Veerman, J. A.; Garcia-Parajo, M. F.; Rensen, W. H. J.; Van Hulst, N. F. *Ultramicroscopy* **1998**, *71*, 149-57.

(14) Cordone, L.; Cupane, A.; Leone, M.; Vitrano, E. *Biophys. Chem.* **1986**, *24*, 259-75.

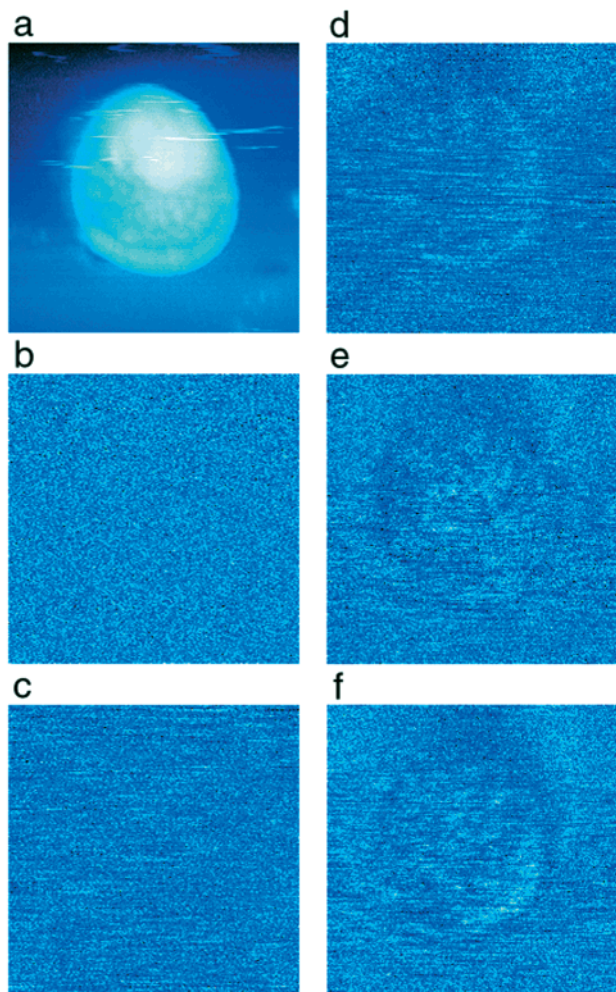


Figure 2. THG NSOM images of a human erythrocyte. (a) Topography and (b–e) THG NSOM images of a human erythrocyte in a $(13.5 \mu\text{m})^2$ area produced at $3\omega = 490, 460, 440, 430$, and 420 nm, respectively. THG contrast increases as the 3ω resonance is tuned to the Soret transition of oxyhemoglobin. Red blood cells can be identified topographically due to their colloidal properties of all being the same size. THG contrast increases as 3ω becomes resonant with the strong Soret transition of oxyhemoglobin. This wavelength study was performed without any reoptimization of the optical signal to both sample the same intensity region of the excitation beam and maintain a constant scan to scan laser–probe geometry. Brighter areas in the optical images correspond to higher THG signals (~ 120 photons/pixel) while darker areas correspond to lower signals (~ 40 photons/pixel). The maximum topographic height of (a) is $0.58 \mu\text{m}$.

Hemoglobin is a protein that is free in the cytoplasm and, therefore, constitutes a bulk probe.

RESULTS AND DISCUSSION

Panels b–f of Figure 2 show near-field THG optical images produced at $3\omega = 490, 460, 440, 430$, and 420 nm, respectively, of the same topographic area shown in (a). These highly repeatable images were collected in immediate consecutive order without any signal reoptimization so as not to sample different areas of the focal region. It is apparent in the image sequence that no contrast is observed when 3ω is off-resonance (b, c), but that significant contrast is observed when 3ω is close (d–f) to the strong Soret transition of oxyhemoglobin shown in Figure 3. It is

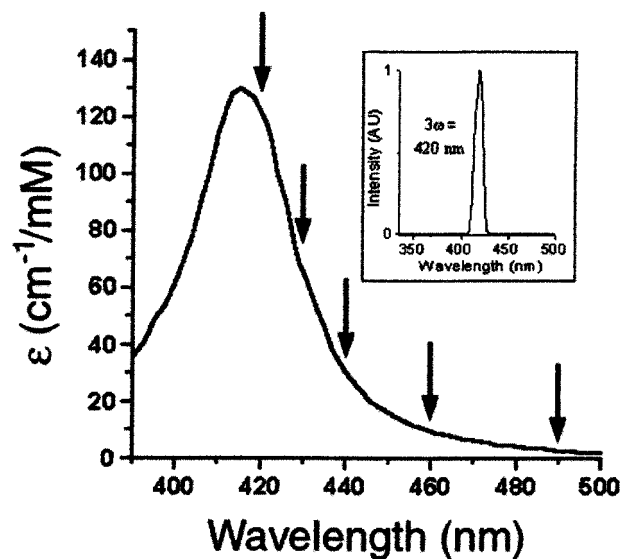


Figure 3. Absorption/THG spectra of oxyhemoglobin. Linear absorption spectrum of oxyhemoglobin in the region of the strong Soret transition. Vertical arrows indicate the experimentally measured 3ω frequencies. The utilization of a 3ω resonance enhancement in THG NSOM imaging, rather than an ω or 2ω enhancement, may have been helpful in preventing damage to the sample via multiphoton ionization mechanisms.¹⁷ The inset shows a spectrum collected through the near-field probe of the 3ω signal at 420 nm to clearly demonstrate that the collected signals were THG. The spectrum was produced via integration of 25 000 laser shots on the CCD.

important to note that strong THG signals were collected in all of the THG images¹⁵ but that image contrast is only observable under resonant conditions in the near-field. It is possible that this background results from third harmonic signals generated from air or from the area of the fiber-optic tip that is within the focal volume of the laser. It should also be noted that hemoglobin, whether oxygenated or deoxygenated, is a nonfluorescent chromophore¹⁶ so that three-photon fluorescence signals were not of concern.

When 3ω overlaps with the strong absorption feature of oxyhemoglobin, as it is in Figure 2d–f, observable contrast is generated in the erythrocyte image. The wavelength dependence of this contrast is indicative of a resonant enhancement contrast mechanism showing chemical specificity from a native, bulk chromophore. This resonant enhancement is a demonstration of singly resonant THG, as the ω and 2ω frequencies do not coincide with other absorption features of the chromophore.¹⁴ The sample showed no visible sign of damage nor was a reduction of signal over time observed.

It is significant that contrast is not observable in Figures 2b and c in which 3ω is off-resonance with every component of the sample. This lack of contrast supports Barad's arguments that far-field, surface-selective THG experiments conducted under tight focusing conditions generate third harmonic radiation, not via an intrinsic surface-specific mechanism, but rather by interference effects related to phase-match relaxation.² Certainly, if significant surface-enhanced components of $\chi^{(3)}$ did exist, as Tsang proposed,¹ different materials in the sample should have different enhance-

(15) Berkovic, G.; Superfine, R.; Guyot-Sionnest, P.; Shen, Y. R. *J. Opt. Soc. Am. B* **1988**, *5*, 668–73.

(16) Adar, F.; Gouterman, M.; Aronowitz, S. *J. Phys. Chem.* **1976**, *80*, 2184–91.

(17) Chang, C. S.; Stehle, P. *Phys. Rev. Lett.* **1973**, *30*, 1283–5.

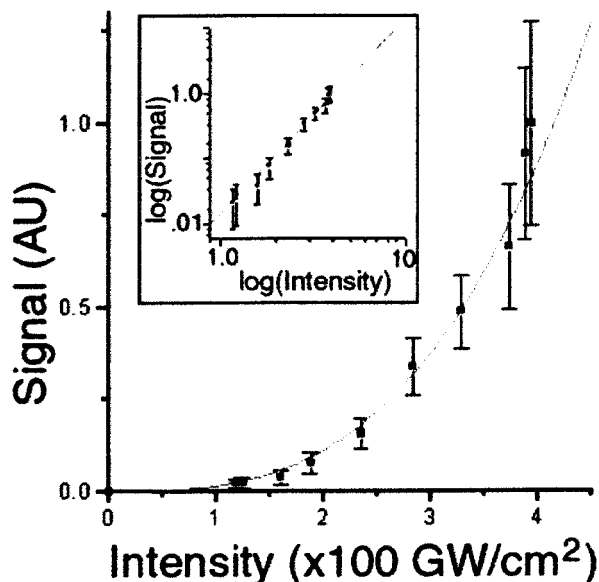


Figure 4. Signal power dependence. Power dependence of the collected signal through the NSOM fiber probe was determined with a variable neutral density filter at $3\omega = 420$ nm. Each data point is the average of 21 000 laser shots. Root-mean-square noise values are shown. The fit to the data points shows a third-order power dependence with fundamental intensity. The inset shows the data represented logarithmically with a linear fit (slope equal to 3) to the data.

ments and produce contrast, although it could be argued that higher signal-to-noise THG NSOM measurements may be required to confirm this finding completely.

Power dependence experiments were also performed using a stepped neutral density filter to be certain that the signal was due to a third-order process. Shown in Figure 4, the collected signal at 10 different intensities indicates a third-order dependence on incident intensity.

The topography and THG NSOM at $3\omega = 420$ nm of two coagulated erythrocytes are shown in panels a and b of Figure 5, respectively. This image demonstrates the highest contrast we have observed so far in THG NSOM imaging. The level of contrast appears to be sensitive to the exact alignment of the laser to the sample and probe. Specifically, higher signal levels often produced less contrast, indicating that the NSOM probe could generate significant background signals when the focus of the laser was more intense on the probe than on the sample. Such background, which was present at similar levels for all of the wavelength studies, remains at a constant level throughout each scan. Thus, the background decreases the signal-to-noise ratio but does not generate contrast.

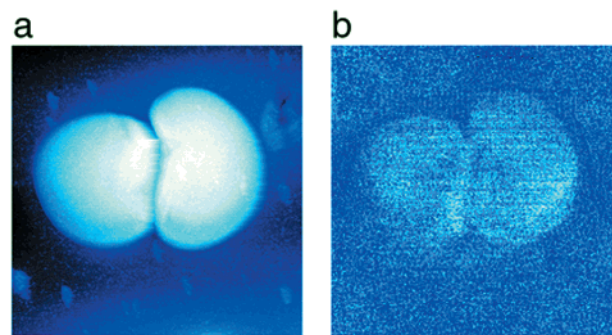


Figure 5. Two red blood cells. (a) Topography and (b) THG NSOM at $3\omega = 420$ nm of a $(17 \mu\text{m})^2$ area showing two coagulated red blood cells. Pixel size is $(85 \text{ nm})^2$. The maximum topographic height of (a) is $0.71 \mu\text{m}$.

This initial demonstration of near-field THG imaging is important in that it provides a means for chemically identifying bulk features in a sample with spatial resolution limited only by the physical dimensions of the NSOM probe. While variations in the nonresonant $\chi^{(3)}$ response associated with interfaces of a sample may provide a separate contrast mechanism for near-field imaging, the resonant $\chi^{(3)}$ response should be more useful since it is chemically specific and more practical since it produces a signal that is typically orders of magnitude stronger. Utilization of resonant enhancement of the third harmonic, as it is chemically specific, removes the need to manipulate and contaminate samples with fluorescent labels. Also, because near-field SHG remains highly surface specific, THG and SHG can be used in a complementary fashion to separately and simultaneously image both bulk and surface environments with chemical selectivity. THG NSOM can also provide insight into the physical nature of the tightly focused, off-resonance experiments due to the a priori relaxation of phase-matching conditions in the near-field. Our current results favor Barad's proposed mechanism of tightly focused far-field THG surface selectivity, which does not involve a true surface effect, but rather indicates that such experiments are a bulk probe.

ACKNOWLEDGMENT

This work was supported by the Experimental Physical Chemistry Division of the National Science Foundation. We also acknowledge the Keck Foundation for supporting the UCB/UCLA Joint Institute for Chemical Imaging Ultramicroscopy.

Received for review June 16, 2000. Accepted August 31, 2000.

AC000699R